Impact of Actuator Torque Density on Expected Robot Life - A Dynamic Model

Gregory Zancewicz
Motus Labs
Dallas, Texas, United States
greg.zancewicz@motus-labs.com

Carlos Hoefken
Motus Labs
Dallas, Texas, United States
carlos.hoefken@motus-labs.com

***Abstract*—Electric actuators not only add weight along an articulated robot arm, but they also have torque and speed limits that impose additional dynamic constraints. Further, the useful life of a robot depends on the extent to which each actuator operates at or near its torque ratings. Cumulative damage theory offers some means of quantifying how much wear a robot arm will sustain in real time as it executes a given trajectory. The dynamic performance as well as fatigue wear of a hypothetical dual-link robot arm are examined in the context of actuator torque density - the actuator's torque-to-mass ratio. The results show that the expected wear to the most stressed joint are approximately inversely proportional to the actuator's torque density. The model also suggests how expected robot life under one or more pre-defined trajectories could be used as an additional constraint in robot arm design and actuator choice.**

***Index Terms*—manipulators, manipulator dynamics, robot motion, robot kinematics, mechatronics, intelligent actuators, electromechanical systems, reliability, reliability engineering, reliability theory, motion control, motion planning, path planning**

I. Introduction

Articulated robot joints employ *actuators* that come with torque ratings that are given in the context of actuator lifetime (e.g. 50 Nm for 1 billion input cycles). Thus, there is an unavoidable intersection of robot design with reliability engineering: the value of torque available from a robotic joint is only meaningful in the context of how many times it can be applied.

In this paper we attempt to examine actuator weight and available torque as not only dynamic constraints (Section III) but also as key drivers for the useable lifetime of the robot (Section IV). We offer a reliability component that could augment the standard robot dynamics model and offer some observations about how such a model could, among other things, aid in optimizing the design of robot arms intended for a limited set of tasks.

II. Actuator Torque Constraints

A. Torque Ratings

The torque available from revolute robotic joints is often specified in terms of *rated*, *maximum repeated peak*, and *maximum peak* torques. These ratings are given in the context of the maximum number of motor cycles a certain fraction of actuators under test are expected to survive before fatigue failure. Generally the fraction considered is 10% and the fatigue lifetime is denoted by L_{10}.

The vast majority of articulated robot arms employ electric actuators with a transmission of some sort integrated with the joint's motor. These transmissions are referred to variously as *gear drives*, *speed reducers*, *gear boxes*, or *gearheads*. Depending on the arm design, they provide reduction ratios (*gear ratios*) ranging from 50 to 160:1. For example, an actuator able to provide 100 Nm of repeated peak torque might employ a transmission with a 100:1 gear ratio and a motor with a repeated peak torque rating of 1 Nm.

B. Torque Density

As one might expect, the more torque that an actuator is called on to produce, the larger and heavier it becomes. As is shown in Figure 1 for a leading brand of commercial actuators, the relationship between actuator mass, m_a, and maximum available torque, T_a, tends to be linear:

$$T_a = T_{a0} + T_{a0}{}' m_a \tag{1}$$

The actuators depicted are full-featured, including motor, transmission, encoder, brake, bearings, and all necessary physical interfaces. Figure 2 shows the relationship between *torque density* - mass per unit torque - and maximum repeated torque:

$$\tau_d(m_a) = \frac{T_a}{m_a} = \frac{T_{a0}}{m_a} + T_{a0}{}' \tag{2}$$

where m_a is the actuator mass and T_a is the maximum repeated torque rating of the actuator.

III. Dynamic Limitations due to Actuator Torque Density

A. Basic Dynamic Model

Figure 3 shows a simple dual-link robotic arm. A first cut of a dynamic performance model for this arm would be:

$$\mathbf{T} = \mathbf{M}(\mathbf{q})\ddot{\mathbf{q}} + \mathbf{C}(\mathbf{q}, \dot{\mathbf{q}})\dot{\mathbf{q}} + \mathbf{G}(\mathbf{q}) \tag{3}$$

where:

$$\mathbf{T} = [\,T_1 \;\; T_2\,]^{\mathrm{T}} \tag{4}$$

$$\mathbf{q} = [\,q_1 \;\; q_2\,]^{\mathrm{T}} \tag{5}$$

with T_1 and T_2 representing the torque applied at joint J_1 and J_2, respectively. The elements of inertia matrix $\mathbf{M}(\mathbf{q})$, Coriolis matrix $\mathbf{C}(\mathbf{q}, \dot{\mathbf{q}})$, and gravity vector $\mathbf{G}(\mathbf{q})$ in terms of

978-1-7281-6790-9/20/$31.00 ©2020 IEEE

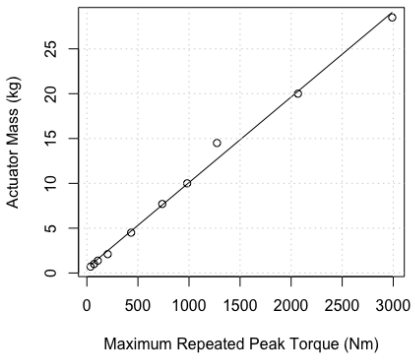

Fig. 1. Mass-torque relation for one commercial actuator line (100:1 gear ratio).

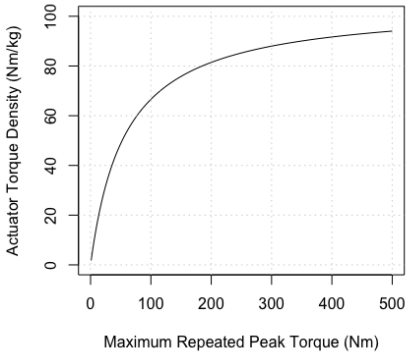

Fig. 2. Torque density characteristics.

link masses m_1 and m_2, link lengths l_1 and l_2, and J_2 actuator parameters m_a, I_a, and ρ_a, are given in an appendix, where m_a is the actuator mass, I_a is the actuator rotational moment of inertia, and ρ_a is the actuator transmission gear ratio. In the discussion that follows, link mass is assumed to be uniformly distributed.

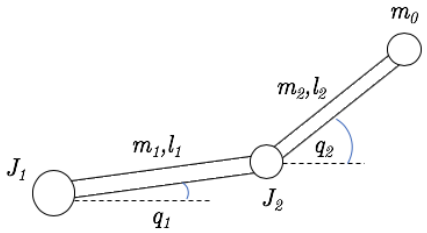

Fig. 3. Dual link robot arm model.

The actuator torques and J_2 actuator mass, m_a, are related (see appendix):

$$\frac{\partial}{\partial m_a}\mathbf{T} = \begin{bmatrix} {l_1}^2\ddot{q}_1 - l_1 g\cos q_1 \\ 0 \end{bmatrix} \tag{6}$$

B. Accounting for Wrist Actuator Mass

The arm model shown in Figure 3 shows a static payload, m_0, but most articulated robots include one or two wrist actuators. To account for this, we can model the payload mass:

$$m_0 = {m_0}' + m_w \tag{7}$$

where ${m_0}'$ represents a true static payload and m_w represents the mass of any wrist actuators. The relationship between the mass of the wrist actuators and $\mathbf{T}$ is:

$$\frac{\partial}{\partial m_w}\mathbf{T} = \frac{\partial}{\partial m_0}\mathbf{T} = \mathbf{M}_{m_0}(\mathbf{q})\ddot{\mathbf{q}} + \mathbf{C}_{m_0}(\mathbf{q},\dot{\mathbf{q}})\dot{\mathbf{q}} + \mathbf{G}_{m_0}(\mathbf{q}) \tag{8}$$

where (see appendix):

$$\begin{aligned} \mathbf{M}_{m_0} &= \frac{\partial \mathbf{M}}{\partial m_0} \qquad (9)\\ &= \begin{bmatrix} {l_1}^2 + {l_2}^2 + 2l_1 l_2\cos q_2 & {l_2}^2 + l_1 l_2\cos q_2 \\ {l_2}^2 + l_1 l_2\cos q_2 & 0 \end{bmatrix} \\ \mathbf{C}_{m_0} &= \frac{\partial \mathbf{C}}{\partial m_0} \qquad (10)\\ &\quad -l_1 l_2\sin q_2 \begin{bmatrix} 0 & 2\dot{q}_1 + \dot{q}_2 \\ \dot{q}_1 & 0 \end{bmatrix} \\ \mathbf{G}_{m_0} &= \frac{\partial \mathbf{G}}{\partial m_0} = -(l_1 + l_2) g\cos(q_1 + q_2)\begin{bmatrix} 1 \\ 1 \end{bmatrix} \qquad (11) \end{aligned}$$

C. Accounting for Actuator Torque Density

We say that the above model is a *first cut* because it does not consider the maximum torques and speeds available from each joint actuator. Thus, the following constraints must be imposed:

$$\begin{aligned} T_1 &\leq T_{1,max} && (12)\\ T_2 &\leq T_{2,max} && (13)\\ \dot{q}_1 &\leq \omega_{1,max}/\rho_1 && (14)\\ \dot{q}_2 &\leq \omega_{2,max}/\rho_2 && (15)\\ & && (16) \end{aligned}$$

where $\omega_{1,max}$ and $\omega_{2,max}$ are the maximum motor speeds available from the actuators at J_1 and J_2, and ρ_1 and ρ_2 are the respective transmission gear ratios.

In the case of J_2, following (2):

$$T_{2,max} = \tau_d(m_a)\cdot m_a \tag{17}$$

There is a similar relation for $T_{1,max}$, but since the mass of actuator at J_1 does not impact the overall arm dynamic model, we will consider $T_{1,max}$ without regard to torque density.

IV. Fatigue Life Model

A. L_{10} lifetime

The fatigue life of transmissions can generally be modeled [5]:

$$L = \left(\frac{T_C}{|T|}\right)^p \tag{18}$$

where L is expressed in terms of either input or output cycles (revolutions), T_C is the *torque capacity* of the unit, and T is the load torque under test. As discussed above, most commercially available actuators and actuator components are specified in terms of L_{10} lifetime - the time by which 10% of a population is expected to have failed. L_{10} lifetimes are usually specified at at least two load torques, generally a *rated torque* (T_R) and a *maximum repeated torque* (T_{MR}). Exponent p and torque capacity T_C can be estimated from any two of these - for example:

$$p = \ln\frac{L_{10,R}}{L_{10,MR}} \Big/ \ln\frac{T_{MR}}{T_R} \tag{19}$$

$$T_C = {L_{10,R}}^{1/p}\, T_R = {L_{10,MR}}^{1/p}\, T_{MR} \tag{20}$$

B. Cumulative Damage

Cumulative damage relates to the concept of a *damage fraction*, which describes the fraction of the fatigue life of a unit consumed prior to failure (see, e.g., [6]). For a unit with fatigue life of L, the damage fraction that results when N of L cycles have passed is:

$$\mathcal{D} = \frac{N}{L} \tag{21}$$

As explained above, however, fatigue life L varies with load, so that each load (torque in our case), T_i, imposes a different damage fraction, D_i for a given number of cycles. The *Palmgren-Miner rule* [7] [8] presumes that failure occurs when:

$$\sum_{i=1}^{n} \mathcal{D}_i = \sum_{i=1}^{n} \frac{N_i}{L_i} = 1 \tag{22}$$

In essence, the device fails when all of its lives are used up.

The number of incremental cycles which occur in some small time interval dt is given by:

$$dN = \frac{|\dot{q}|}{2\pi}\, dt \tag{23}$$

Following (18):

$$d\mathcal{D} = \left(\frac{|T|}{T_C}\right)^p \frac{|\dot{q}|}{2\pi}\, dt \tag{24}$$

so that the cumulative damage sustained between times t_1 and t_2 is:

$$\mathcal{D} = \frac{1}{2\pi {T_C}^p} \int_{t_1}^{t_2} |T|^p\, |\dot{q}|\, dt \tag{25}$$

V. Robot Arm Simulation

A. Robot Arm Parameters

In order to consider the practical implications of what has been discussed above, we will consider a hypothetical robot arm executing a repeated vertical trajectory, such as might be required in a painting and welding task (see Figure 4). The robot arm operates in the vertical (xz) plane and comprises two links and four actuators (base, elbow and two wrist), with parameters:

$$\begin{aligned} m_1 &= 20 \text{ kg} \\ m_2 &= 10 \text{ kg} \\ l_1 &= 100 \text{ cm} \\ l_2 &= 50 \text{ cm} \\ T_{1,max} &= 230 \text{ Nm} \\ T_{2,max} &= 230 \text{ Nm} \\ \omega_{1,max} &= 5 \text{ rad/s} \\ \omega_{2,max} &= 5 \text{ rad/s} \\ m_a &= 5 \text{ kg} \\ I_a &= 4 \text{ kg cm}^2 \\ \rho_a &= 100 \\ m_w &= 7 \text{ kg} \end{aligned}$$

The above parameters follow closely those supported by 100:1 gear ratio size 17 and size 25 actuators available from one leading commercial supplier. The trajectory of the tip of the arm is given by:

$$\mathbf{r}(t) = \hat{x}\, x_0 + \hat{z}\, (z_0 + \dot{z}_0 t) \tag{26}$$

where $\hat{x}$ and $\hat{z}$ are Cartesian unit vectors.

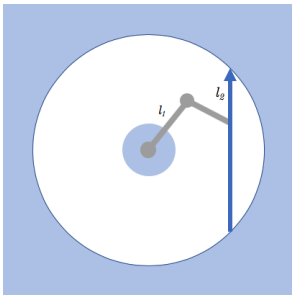

Fig. 4. Robot arm executing a repeated vertical trajectory.

The trajectory example considered in this text is relatively simple. Examples of more complex trajectories for various types of articulate robot arms can be found in [1]- [4].

B. Actuator Lifetime Model

Based on typical gear drive life specifications, an exponent of $p = 2.7$ is assumed for the L_{10} life relation of the elbow actuator, and a lifetime of 10^8 input cycles is assumed at the maximum repeatable peak torque. In actuality, these values may vary somewhat from what we are assuming, but this

will not affect the basic implications of the simulation result. Following (20):

$$\begin{aligned} T_C &= {L_{10,MR}}^{1/p} \cdot T_{MR} \\ &= \left(10^8\right)^{1/2.7} \cdot 230 \text{ Nm} \\ &\approx 210 \text{ kNm} \end{aligned}$$

C. Simulation Results

1) Nominal Torque Density: Figures 5 through 7 show the dynamic behavior of the arm during the operation with:

$$\begin{aligned} x_0 &= 1 \text{ m} \\ z_0 &= -1 \text{ m} \\ \dot{z}_0 &= 1 \text{ m/s} \end{aligned}$$

Figure 5 shows the angles of joints J_1 and J_2 throughout the time of the reference trajectory. Figure 6 shows the corresponding angular velocities. Figure 7 shows how the applied torques at each joint develop, as calculated using (3). Figure 8 shows the calculated instantaneous L_{10} lifetime - i.e. how many cycles a new unit could sustain if operated at the corresponding instantanous torque indefinitely. What is of more practical importance, however is how much fatigue wear (or damage) the arm sustains as a result of the operation, as expressed by (25). As is seen in Figure 9, the actuator at J_2 experiences roughly four times the wear of the actuator at J_1 for this particular trajectory.

2) Improved Torque Density: Figures 10 through 12 illustrate impact to arm dynamics and fatigue wear when the torque density of the elbow and wrist actuators are doubled:

$$\begin{aligned} m_a &= 5 \text{ kg} \longrightarrow 2.5 \text{ kg} \\ m_w &= 7 \text{ kg} \longrightarrow 3.5 \text{ kg} \end{aligned}$$

Since the predicted wear for J_2 is much higher than that for J_1, only J_2 values are shown. Figure 10 shows that the decrease in weight leads to a 30% reduction in the amount of torque that J_2 needs to deliver. This leads to a higher instantaneous L_{10} for each point along the trajectory (Figure 11), which in turn lowers the cumulative damage sustained by the joint. As seen in Figure 12, the fatigue wear at J_2 drops by almost 50%.

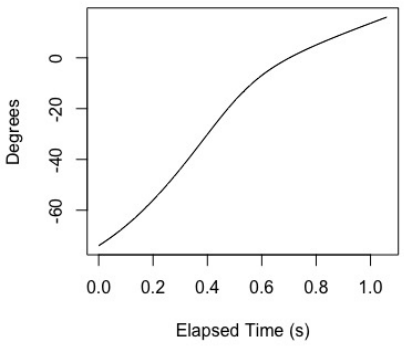

(a) J_1

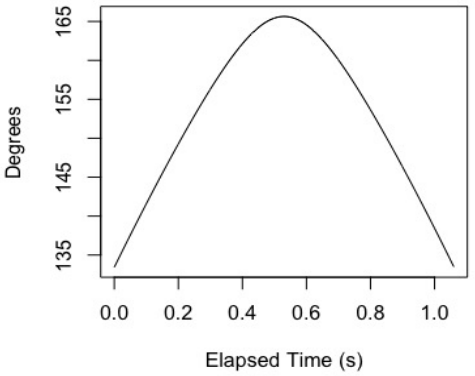

(b) J_2

Fig. 5. Joint angles for reference trajectory.

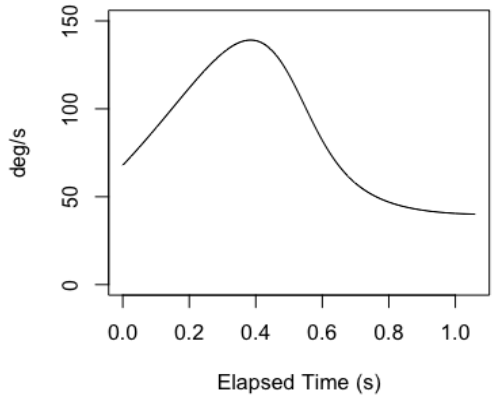

(a) J_1

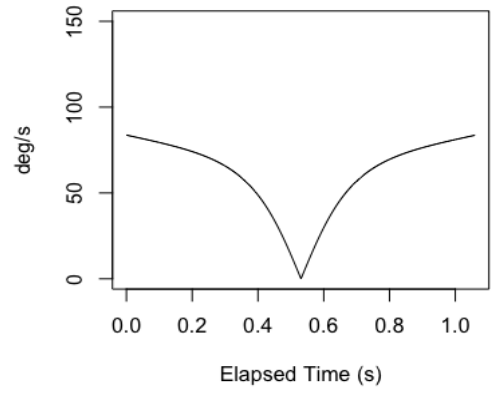

(b) J_2

Fig. 6. Joint velocities for reference trajectory.

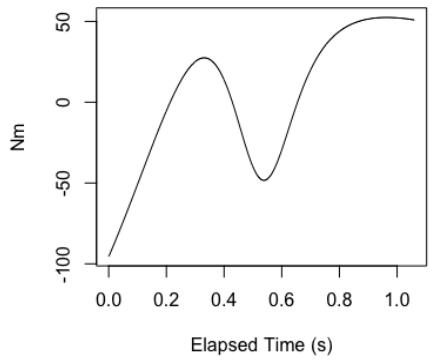

(a) J_1

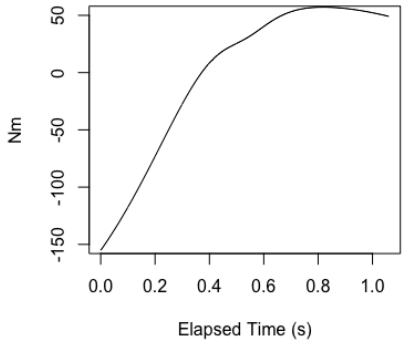

(b) J_2

Fig. 7. Joint torques required for reference trajectory (nominal actuator torque density).

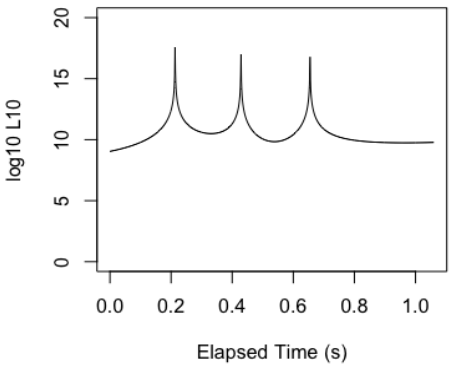

(a) J_1

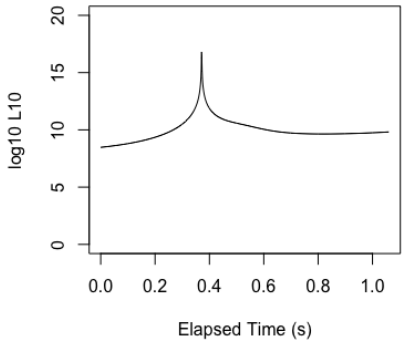

(b) J_2

Fig. 8. Instantaneous L_{10} fatigue life of joint actuators (nominal actuator torque density).

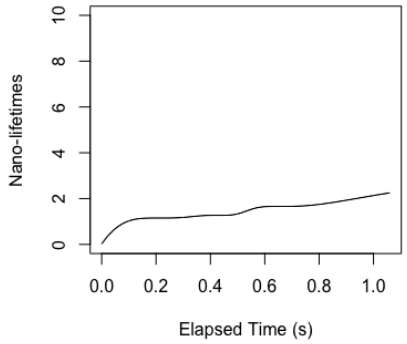

(a) J_1

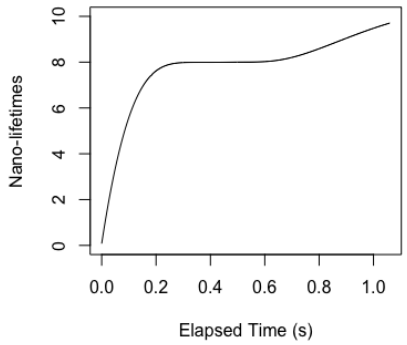

(b) J_2

Fig. 9. Cumulative damage to each joint sustained during one operation (nominal actuator torque density).

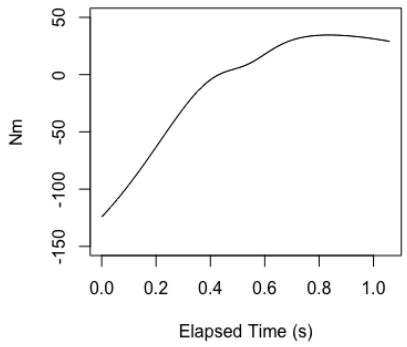

Fig. 10. J_2 torque required for reference trajectory (2X nominal actuator torque density).

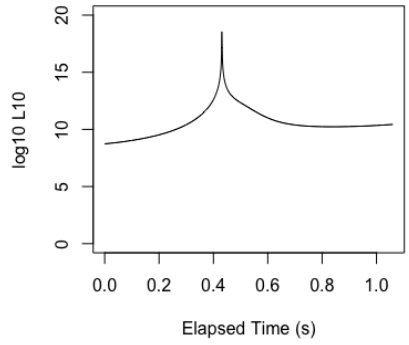

Fig. 11. Instantaneous L_{10} fatigue life of J_2 actuator (2X nominal actuator torque density).

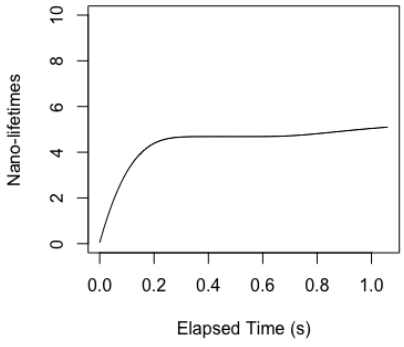

Fig. 12. Cumulative damage sustained by J_2 during one operation (2X nominal actuator torque density).

VI. Discussion and Conclusions

A few observations might be made with regard to the results in the previous section:

- The fatigue wear to individual joints was calculated, but these results were not interpreted to provide an estimate of the fatigue life of the robot. This can be accomplished by recasting p and T_C in the lifetime relation (18) of each actuator into Weibull shape and scale parameters for individual actuator probability distribution functions [9], and then using the individual pdf's to estimate L_{10} for the robot. In our case the fatigue wear to J_2 was dominant, but when wear is closer to parity the individual pdf's must be considered.
- The results of the previous section were for one specific trajectory. Depending on what other trajectories might be employed, some other torque pattern, and hence wear trend, should be expected. This can be seen explicitly in the dependencies of $\mathbf{T}$ expressed in (6) and (8).
- By the same token, (3) implies that a different choice of link lengths, l_1 and l_2, could still allow the arm to execute the trajectory in (26), but with a completely different torque profile and hence, in general, a different expected arm lifetime. By extension, if one is to go about configuring a robot arm to complete a single task repeatedly, a lifetime-optimized design might yield a different choice of link lengths than those one might otherwise choose.
- The simulations above looked at the impact of doubling the actuator torque density. Other simulations were carried out using the same arm configuration and trajectory, but with torque densities ranging from 1X nominal to 2X nominal. The empirical trend observed was:

$$\mathcal{D}_r \approx \tau_r^{-\gamma} \tag{27}$$

where in this case $\gamma = 0.9873$ (see Figure 13).
- The trend shows that reducing the weight of even a part of the actuator can have a dramatic positive impact on the lifetime of the most stressed joint. If, for example, the gearbox comprises 30-40% of the actuator weight, then doubling the torque density of just the gearbox would increase the torque density of the actuator by 15-20%, which could lengthen its lifetime by 10-20%.

Appendix A
Dual Link Robot Arm Torque Equations

A. Robot Equation

$$\mathbf{T} = \mathbf{M}(\mathbf{q})\ddot{\mathbf{q}} + \mathbf{C}(\mathbf{q}, \dot{\mathbf{q}})\dot{\mathbf{q}} + \mathbf{G}(\mathbf{q}) \tag{A.1}$$

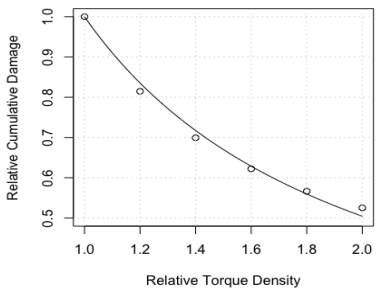

Fig. 13. Cumulative damage reduction as a function of actuator torque density improvement for preceding scenario.

$$\mathbf{T} = [\, T_1 \; T_2 \,]^{\mathrm{T}} \tag{A.2}$$

$$\mathbf{q} = [\, q_1 \; q_2 \,]^{\mathrm{T}} \tag{A.3}$$

$$|T_1| \leq T_{1,max} \tag{A.4}$$

$$|T_2| \leq T_{2,max} \tag{A.5}$$

$$|\dot{q}_1| \leq \omega_{1,max}/\rho_1 \tag{A.6}$$

$$|\dot{q}_2| \leq \omega_{2,max}/\rho_2 \tag{A.7}$$

B. Inertia Matrix

$$\mathbf{M}(\mathbf{q}) = \begin{bmatrix} M_{11}(\mathbf{q}) & M_{12}(\mathbf{q}) \\ M_{12}(\mathbf{q}) & M_{21}(\mathbf{q}) \end{bmatrix} \tag{A.8}$$

$$\begin{aligned} M_{11}(\mathbf{q}) = {} & \frac{1}{3} m_1 {l_1}^2 \\ & + m_2 \left({l_1}^2 + \frac{1}{3} {l_2}^2 + l_1 l_2 \cos q_2 \right) \\ & + m_0 \left({l_1}^2 + {l_2}^2 + 2 l_1 l_2 \cos q_2 \right) \\ & + m_a l_1^2 \end{aligned} \tag{A.9}$$

$$\begin{aligned} M_{12}(\mathbf{q}) = {} & \frac{1}{2} m_2 \left(\frac{2}{3} {l_2}^2 + l_1 l_2 \cos q_2 \right) \\ & + m_0 ({l_2}^2 + l_1 l_2 \cos q_2) \end{aligned} \tag{A.10}$$

$$M_{21}(\mathbf{q}) = M_{12}(\mathbf{q}) \tag{A.11}$$

$$M_{22}(\mathbf{q}) = \frac{1}{3} m_2 {l_2}^2 + I_a \rho_a^2 \tag{A.12}$$

C. Coriolis Matrix

$$\begin{aligned} \mathbf{C}(\mathbf{q}, \dot{\mathbf{q}}) = {} & - \left(\frac{1}{2} m_2 + m_0 \right) l_1 l_2 \sin q_2 \\ & \cdot \begin{bmatrix} 0 & 2\dot{q}_1 + \dot{q}_2 \\ \dot{q}_1 & 0 \end{bmatrix} \end{aligned} \tag{A.13}$$

D. Gravity Vector

$$\mathbf{G}(\mathbf{q}) = [\, T_{1g} \; T_{2g} \,]^{\mathrm{T}} \tag{A.14}$$

$$\begin{aligned} T_{1g} = {} & - \left(\frac{1}{2} m_1 + m_a \right) l_1 g \cos q_1 \\ & - \left[(m_0 + m_2) l_1 + \left(m_0 + \frac{1}{2} m_2 \right) l_2 \right] \\ & \cdot \; g \cos(q_1 + q_2) \end{aligned} \tag{A.15}$$

$$\begin{aligned} T_{2g} = {} & - \left[(m_0 + m_2) l_1 + \left(m_0 + \frac{1}{2} m_2 \right) l_2 \right] \\ & \cdot \; g \cos(q_1 + q_2) \end{aligned} \tag{A.16}$$

Derivations of the above can be found in [10] though [13].

REFERENCES

[1] A. Sutapun and V. Sangveraphunsiri, "A 4-DOF Upper Limb Exoskeleton for Stroke Rehabilitation: Kinematics Mechanics and Control," *International Journal of Mechanical Engineering and Robotics Research*, Vol.4, No. 3, pp. 269-272, July 2015.

[2] P. S. Rao and N. M. Rao, "Position Analysis of Spatial 3-RPS Parallel Manipulator," *International Journal of Mechanical Engineering and Robotics Research*, Vol. 2, No. 2, pp. 80-90, April 2013.

[3] Z. H. Ang, C.K. Ang, W H. Lim, L. J. Yu, and M.I. Solihin, "Development of an Artificial Intelligent Approach in Adapting the Characteristic of Polynomial Trajectory Planning for Robot Manipulator," *International Journal of Mechanical Engineering and Robotics Research*, Vol. 9, No. 3, pp. 408-414, March 2020.

[4] M Nazemizadeh, M Taheri, and S. Nazeri, "Dynamic Modeling and Path Planning of Flexible-Link Manipulators," *International Journal of Mechanical Engineering and Robotics Research*, Vol. 3, No. 2, pp. 223-228, April 2014.

[5] Bloch and Geitner, *Practical Machinery Management for Process Plants, Volume 2: Machinery Failure Analysis and Troubleshooting*, 1997.

[6] Hashin and Rotem, "A Cumulative Damage Theory of Fatigue Failure", Scientific Report No. 3, Department of Solid Mechanics, Materials and Structures, Tel Aviv University, February 1977.

[7] A. Z. Palmgren, "Die Lebensdauer von Kugellagern", *Zeitschrift des Vereins Deutscher Ingenieure*, vol. 68, p.339ff., 1924.

[8] M. A. Miner, "Cumulative Damage in Fatigue," *Journal of Applied Mechanics*, vol. 12, p.A139ff., 1945.

[9] T. A. Harris and M. N. Kotzalas, *Advanced Concepts of Bearing Technology* (5th ed.), CRC Press, 2007, p.319ff.

[10] B. K. P. Horn, "Kinematics, Statics, and Dynamics of Two-D Manipulators," MIT Artificial Intelligence Laboratory Working Paper 99, June 1975.

[11] E. I. Rivin, *Mechanical Design of Robots*, McGraw Hill, 1988.

[12] H. Choset *et al.*, *Principles of Robot Motion: Theory, Algorithms, and Implementations*, MIT Press, 2005.

[13] L. Sciavicco and B. Siciliano, *Modelling and Control of Robot Manipulators*, Springer, 2000.

[14] M. W. Spong, S. Hutchinson, and M. Vidyasagar, *Robot Modeling and Control*, Wiley, 2020